FISEVIER

Contents lists available at ScienceDirect

International Journal of Electronics and Communications

International Journal Of Electronics and Communications

journal homepage: www.elsevier.com/locate/aeue

Regular paper

Modal analysis-based ultrawideband 4×4 MIMO antenna with flower configuration

Ankireddy Chandra Suresh ^a, Chandraiah.G ^b, Chiranjeevi Althi ^c, Om Prakash Kumar ^{d,*}, Moath Alathbah ^e, BTP Madhav ^f

- a Department of Electronics and Communication Engineering, Sri Vasavi Institute of Engineering & Technology Nandamuru Pedana Mandal A.P India
- ^b Department of Electronics and Communication Engineering, Sri Venkateswara College of Engineering Tirupathi A.P India
- ^c Department of Electronics and Communication Engineering, SV University College of Engineering, SV University Tirupathi A.P India
- d Department of Electronics and Communication Engineering, Manipal Institute of Technology, Manipal Academy of Higher Education, Manipal 576104, India
- e Department of Electrical Engineering, College of Engineering, King Saud University, Riyadh 11451, Saudi Arabia
- f Department of ECE, ALRC R&D, Koneru Lakshmaiah Education Foundation, Vaddeswaram, AP, India

ARTICLE INFO

Keywords: CMA Isolation UWB MIMO

ECC CCL MEG

ABSTRACT

This paper presents a novel UWB MIMO antenna with a flower-like configuration. The antenna design incorporates a circular-shaped stub on the ground, which enhances isolation from 3.1 GHz to 11 GHz and provides an impressive impedance bandwidth of 117.8 %. The proposed MIMO antenna consists of four radiating elements arranged in a flower pattern, with the elements oriented orthogonally, on a substrate measuring $40 \times 40 \times 1.6$ mm³. This quad-port MIMO system achieves a peak gain of 5.5 dBi and a radiation efficiency of 90 %. The isolation between ports is maintained below 26 dB, while the Envelope Correlation Coefficient (ECC) is 0.0116, and the Diversity Gain (DG) is 10 dB. The system also exhibits a Channel Capacity Loss (CCL) of less than 0.32 bits/sec/Hz and a Mean Effective Gain (MEG) of less than -3.3 dB. These results highlight the antenna's suitability for use in high-speed UWB portable applications.

1. Introduction

Affordable, multi-purpose, small antennas are desperately needed in the current wireless communication environment. To address this need, several technologies have been developed. Ultra-wideband (UWB) technology evolved with the FCC's allocation of frequency limits from 3.1 GHz to 10.6 GHz for common utilization. The current state of wireless communication greatly necessitates the need for multifunctional, reasonably priced, small antennas. Numerous technologies have been developed to meet this demand. Its Key features include minimum power consumption, more data rates, an extensive range of frequencies, and economic effectiveness. These attributes have drawn significant interest from researchers in designing UWB antennas for portable devices [1]. The primary goal is to create an antenna radiator that is optimized for the broad UWB frequency spectrum. Furthermore, it's crucial to design UWB antenna beam-forming systems incorporating diverse UWB gears like transitions, hybrid couplers, crossovers, hybrid couplers, feed networks, and phase shifters, ensuring all elements are accurately aligned to meet UWB standards [2]. Thus, utilizing UWB-

MIMO technology presents a promising solution for enhancing data rates while maintaining low power requirements [3]. Despite their numerous benefits, MIMO systems come with several challenges that require careful attention. One of these issues is to keep the overall design compact while still providing good performance. Greater compactness leads to higher mutual coupling from current flow between the ports, which negatively impacts DG, and operational characteristics. Proper isolation between antenna elements is required to avoid excessive mutual interaction. Researchers have investigated and proposed a variety of approaches for improving isolation between antenna elements [4]. These approaches include Defected Ground Structures (DGS) stub loading, Neutralization Lines (NLs), metamaterial-based isolators, and parasitic materials Several research in the literature have addressed both compactness and mutual coupling concerns concurrently [5]. A novel method is used to design 4×4 MIMO, in that integrate symmetric layout and orthogonal structure. A novel decoupling technique is called multislit and multi slot is used to achieved isolation more than 22 dB in UWB range. Moreover, this technique efficiently miniaturizes the size of the antenna and broadens its IBW [6]. The four radiators of the UWB-MIMO

E-mail address: omprakash.kumar@manipal.edu (O.P. Kumar).

https://doi.org/10.1016/j.aeue.2025.155685

Received 28 November 2024; Accepted 13 January 2025 Available online 27 January 2025

^{*} Corresponding author.

are arranged orthogonally to one another. Every radiator has a stepped micro strip feed line and a cut semicircular patch. To improve isolation, defective ground components on the ground plane are joined by a swastik form. The polarization diversity technique improves the overall isolation by up to 17 Db [7]. In Square shaped conducting patch removed four arcs at the edges to form the single radiator. In this MIMO two radiators are closely placed to achieve the spatial diversity technique and further isolation is enhanced by defected ground technique on ground plane [8].The fractal shaped 2 \times 1 MIMO is designed with a dimensions of 25 \times 35 $\,\mathrm{mm}^2$ and resonated at a frequency of 3.5 GHz. The integration of different strip slots to achieve good radiation and diversity parameters like ECC,DG and MEG [9].

A 4 × 4 MIMO flexible antenna is designed using orthogonal technique to achieve good isolation. The each radiator in MIMO is composed as crescent-shaped monopole and connected to curve shaped waveguide to enhance the isolation. This MIMO utilized the flat and bending layouts to achieve isolation more than 17 dB, gain is 5 dB and ECC is less than 0.01 [10]. A cost-effective 2 \times 2 and 4 \times 4 UWB-MIMO considered with different orientations to minimize the common coupling among the radiating components. The dimensions of 2 \times 2 MIMO is 20 \times 45 mm^2 printed on FR-4 material. The same design procedure was applied for 4 \times 4 MIMO with low ECC. The innovation of this design was no need of special isolation techniques, the orientation of the elements enhance the isolation more than 20 dB [11].A 4 × 4 S-shaped wide band MIMO designed to operate from 25 GHz to 39 GHz. The over all dimensions of MIMO is $24 \times 24 \text{ mm}^2$ and each s-shaped radiator occupied a size of 10 \times 12 mm² dimensions. An innovation decoupling network was used to achieved the isolation more than 26 dB, gain is 7.1 dB and ECC is less than 0.05 [12].A Rogers RT/Durod 5880 substrate used to design lowweight, low cost square loop antenna. This MIMO resonated at 26 GHz and 40 GHz and providing bandwidth of 13 GHz. Each single radiator size is 9 mm \times 11 mm and consist of 3 rectangular square loops with transmission line. The four elements were arranged in traditional way to get gain of 10.1 dB and efficiency of 92 % [13].

A 2 \times 2 UWB-MIMO was designed with dimensions of 52 \times 26 mm2 on RO5880 with a thickness of 0.787 mm. Each radiator was designed with 9 circular springs placed in rectangular patches. The isolation was improved by rectangular slots. The uniqueness of this MIMO was the CPW method which achieved isolation up to 16 dB and bandwidth from 2.3 GHz to 11.5 GHz total 9.2 GHz [14]. The uniqueness of this 4×4 MIMO is that there is no need to add any extra isolation method for reducing mutual coupling. Each radiator in MIMO comprises a fractal circular ring placed on the partial ground to achieve isolation up to 15 dB and bandwidth from 2.67 GHz to 12 GHz [15]. A Compact 4×4 antenna was designed using 40 mm \times 40 mm and exhibited the 11 GHz bandwidth and isolation of more than 17 dB. An asymmetric design technique without any decoupling method is used to get return losses of 10 dB in the entire UWB range [16]. A 4×4 MIMO composed of two identical slot dipoles and planer radiators. The mutual coupling was minimized by utilizing the polarization diversity technique. In addition with that Z-and L-shaped decoupling stubs were used to enhance the isolation up to -17 dB in the UWB spectrum. By using these decoupling networks good diversity and radiation characteristics were achieved

A new method of isolation was introduced to design the 4 \times 4 MIMO-antenna in wireless communication technology. Each radiator in triangular shape and used neutralization ring configuration. The radiators are configured as symmetrical and orthogonal. The novel Neutralization ring used as isolation technique and enhanced the isolation up to 17 dB in entire 3.1 to 17.3 GHz with a gain of 5 dB [18]. The dimensions of the MIMO was $0.67\lambda \times 0.81\lambda \times 0.0028\lambda$ at low cut off frequency of 3.58 GHz.The four port structure is enclosed in octagonal slot with CPW. The ground structure was designed with plus-shaped slots configuration hence this arrangement achieved the isolation of more than 15 dB, efficiency 89 %, and gain was 6.8 dB [19]. A 4 \times 4 CPW MIMO is designed and operated in the dual-band. The CPW designed four radiators and

arranged in orthogonally. A DGS was used to improve the isolation and BW. This arrangement of design produced an ECC below 0.0025 and a DG of nearly 10 dB [20].A 4×4 miniaturized 4×4 MIMO designed for UWB applications and also investigated in L, S, C, and X band frequencies. The overall dimensions were 78 mm \times 50 mm and well operated at 2.02 GHz,5.87 GHz, and 11.9 GHz. This reconfigurable MIMO used the defected ground structure as an isolation method and achieved the isolation up to 18 dB [21]. The 4×4 MIMO with a dimension were 40 \times 40 \times 1.6 mm3 designed to reduce mutual coupling. In this, each radiator's dimensions were reduced by the inclusion of vertical, and horizontal conducting strips and diagonal conducting strips pooled to form a single radiator. All four radiators were arranged orthogonal to each other. A plus-shaped partial ground structure among the elements enhanced isolation by more than 20 dB and offered a bandwidth was 10.2 GHz in the UWB range. This innovative radiating structure produced an ECC < 0.05 and DG of nearly 10 dB. This model is well suited to 5G wearable devices [22]. The challenges in modern communication antennas were wider bandwidth and more isolation. In 4×4 MIMO each radiator is designed by a semicircular radiator included with guitar shape slot and half circle slot. The inserting of slots enhances the isolation and increases the bandwidth. The combination of defected ground structure and parasitic elements minimize the mutual coupling. The innovative isolation technique produced a bandwidth from 4.5 to 16.6 GHz, with an impedance bandwidth of 113 % and isolation of more than 20 dB [23]. A 4×4 MIMO is designed with gap sleeves and H-slots. The designed antenna dimensions are 80×80 \times 1.6 mm 3 using the co-planner waveguide technique. This antenna offered wider bandwidth from 2.1 GHz to 20 GHz and isolation is more than 25 dB. This MIMO achieved good diversity and radiation properties [24]. The dimensions of 4 \times 4 MIMO antenna is 40 \times 40 \times 1.524 mm³ and placed orthogonal to one other. This MIMO achieved bandwidth from (3-13.5 GHz) including UWB (3.1-13.25 GHz), 11 GHz (10.7 to 11.7 GHz) and 13 GHz (12.75 to 13.25 GHz) frequency bands. The four rectangular bricks are arranged below the ground of each radiator to avoid unwanted interference among the MIMO elements. The innovative arrangement of partial ground enhance the radiation and MIMO characteristics [25]. A six-port MIMO antenna designed with a new novel method for UWB applications. Each radiator was in the form of a pyramid and placed in a symmetrical form. To enhance the isolation defected ground structure combined with parasitic elements method. This innovative method produced isolation more than 20 dB from 2.9 to 11 GHz with an impedance bandwidth of 116 % [26].

However, the above mentioned methods do not adequately improve isolation or reduce the ECC (Envelop Correlation coefficient). This paper employs a more advanced approach, characteristic mode analysis, which involves a detailed design process. The CMA is used to Analyze antenna's radiation through its individual modes allows for a better understanding of its key properties. In the proposed design, four flower-shaped radiators achieve polarization diversity with the separate ground structure. The projected four-port antenna spans (3.1–11.5) GHz and offers less interference.

The structure of this article is given as follows: Section 2 presents the characteristic mode evaluation of the proposed antenna. Section 3 details the antenna design methodology. Section 4 covers the results and comparisons of the proposed antenna. Section 5 details the time-domain analysis of the proposed MIMO in different layouts. Section 6. describes the comparisons of the proposed model with active models. And lastly, this article, wrapped with section 7 includes the conclusions of the proposed model.

2. CMA for proposed antenna

The CMA is a robust method used for antenna analysis and design. This approach uses the mathematical decomposition of the antenna into its basic modes to assess its radiation characteristics. The core idea behind CMA is to represent the EM fields of the perfect electric

Table 1Significance of characteristic mode parameters.

| Eigen values (λ_i) | Modal Significance (MS) | $CA(\theta_i)$ | Significance |
|------------------------------|----------------------------|-----------------------------------|----------------------|
| $\lambda_i < 0$ | Ms not equals to one | $180^0 < 	heta_i < 270^0$ | Electrical Energy |
| $\lambda_i = 0$ | Ms equals to one | $\theta_i = 0^0$ | Resonance |
| $\lambda_i > 0$ | Ms not equals to one | $90^0 \!\!<\!\! \theta_i < 180^0$ | Magnetic energy |

Table 2
Measurements of the desired MIMO (in mm).

| Parameter | Symbol | Value | Parameter | Symbol | Value |
|---------------------------|--------|-------|--------------------------------|--------|-------|
| Inner circle Radius | r1 | 1.5 | Length of the ground brick | L4 | 4.2 |
| Outer circle Radius | r2 | 2 | Distance from ground edge | L5 | 3.8 |
| feed width | wf | 1.2 | Outer radius on ground | r4 | 5 |
| Ellipse diameter | D2 | 6 | Inside radius on the ground | r3 | 2 |
| Length of the feed | Lf | 6 | Width of the | Wh | 1.6 |
| Substrate Length | Wl | 40 | substrate | | |
| substrate height | Ws | 40 | | | |
| Width of the ground brick | L3 | 8.4 | | | |

conductor as a sum of its CMs. These modes are unique in that they can radiate independently from one another. Analyzing an antenna's radiation through its modes for a better understanding of its key properties enables performance optimization. In the CMA technique, eigenvalues are solved, and the antenna's characteristic modes are measured. The eigenvalues correspond to the resonant frequencies. A fundamental tenet of CMT states that N transverse eigen currents (Ji), when added together represent the weighted total current generated by an incident EM field on a radiating device.

The shape and material composition of the structure determine these Eigen currents. The total current is shown in equation (1) [27]. The modal weight coefficients (i) influence the contribution of edge currents to the overall current. Each incurrent produces a distinct radiated electric field, which combines to form the complete radiated field.

$$J = \sum_{i=1}^{N} \beta_i J_i \tag{1}$$

The equation (2) can be used to compute the MS [27].

$$M_s = \left| \frac{1}{1 + j\lambda_i} \right| \tag{2}$$

The MS is inversely varied with eigen value and represented in equation (2). The eigenvalue can be determined using [Z] and the eigencurrent, as outlined in equation (3) and (4) [27].

$$[Z] = [R] + j[X] \tag{3}$$

$$[X]J_i = \lambda_i[R]J_i \tag{4}$$

Where R and X stand for the Z matrix's real and imaginary elements. The eigen values are significant because they can be used to anticipate conducting structures' internal energy and resonant frequency depicted in Table 1. The $CA(\theta_1)$ may be found using equation (5) [27].

$$\theta_i = 180^0 tan^-(\lambda_i) \tag{5}$$

3. Design of 4×4 UWB-MIMO antenna

Mounted on an FR-4 surface, the four flower-shaped radiators with $\tan\!\delta\!\!=\!\!0.002$ and a relative permittivity (ϵ_r) of 4.3. The flower-shaped radiator was developed through several adjustments to the circular-radiator.The separation between two adjacent radiators are 11 mm. The antenna's ground plane incorporates a defective ground structure along with a circular-shaped stub to improve isolation. The Proposed MIMO antenna can also work without relying to separate ground plane. But that designed antennas does not cover larger bandwidth and offers less impedance bandwidth (IBW) as well as low isolation.The optimized parameter values are shown in Table 2. By using this dimensions the 4 \times 4 Flower shaped antenna designed using CMA and depicted in Fig. 3.

The ellipse with a dimensions of 1.5 mm radius on x and 3 mm on y axis and placed at height of 16 mm from the bottom of the substrate vertically. Arrange this type of ellipses 45 degrees to vertical ellipse. Total six 8 ellipses are possible at a 45 degrees to one another. Combine this 8 ellipses forms the flower shape. Add feed to the flower shape with length of 6 mm and width of 1.2 mm and resultant is depicted in Fig. 1 (a). Now remove the circular cover with a radius (r2) of 2 mm from the centre of the flower and resultant shape is depicted in Fig. 1(b).Add circular-patch conducting material with a radius (r1) 1.5 mm at the centre of flower the resultant is depicted in Fig. 1(c).Add rectangular brick at bottom of each radiator the resultant is depicted in Fig. 1 (d).

The 4 \times 4 Flower shaped radiator is designed in four stages. The stages of antennas are A#0, A#1, A#2 and A#3. The Four single flower radiator shown in Fig. 1 (a) are arranged orthogonal to one another on 40 \times 40 \times 1.6 mm³ substrate to form the antennaA#0.This resultant antenna A#0 is depicted in Fig. 2 (a). Analyze the CMs of A#0 by applying multilayer solver. Total 10 CMs are generated out 10 modes only four CMs are useful. The CMs CM2, CM4, CM5 and CM6 are located in mid band frequencies (4–8 GHz).The remaining CMs CM1,CM3,CM7, CM8,CM9 and CM10 are not useful. That means Antenna A#0 is well suited at Mid band frequencies and not suited at high and low band frequencies. The modal significances of A#0 are represented in Fig. 4. (a). Apply excitation signal to antenna A#0 and analyze its S-Parameters. The Subsequent S-Parameters of antenna A#0 are depicted in Fig. 5 (a).

Add a rectangular brick to the below of the each flower radiator on

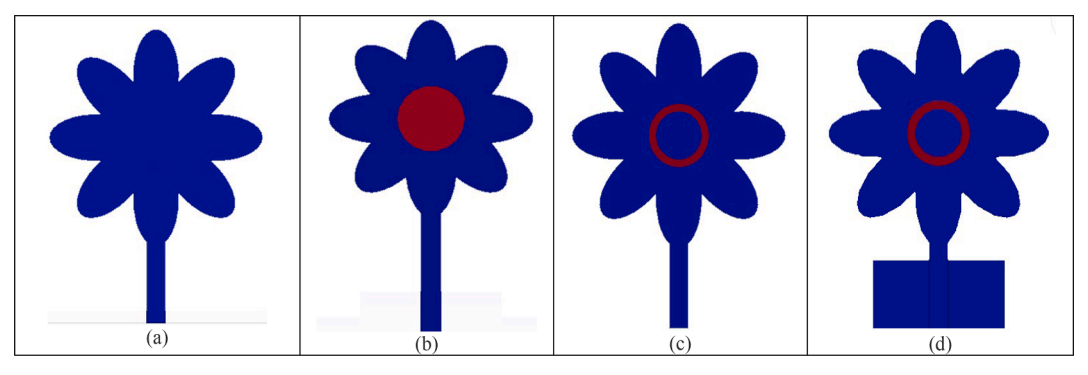


Fig. 1. Evolution of single flower radiator.

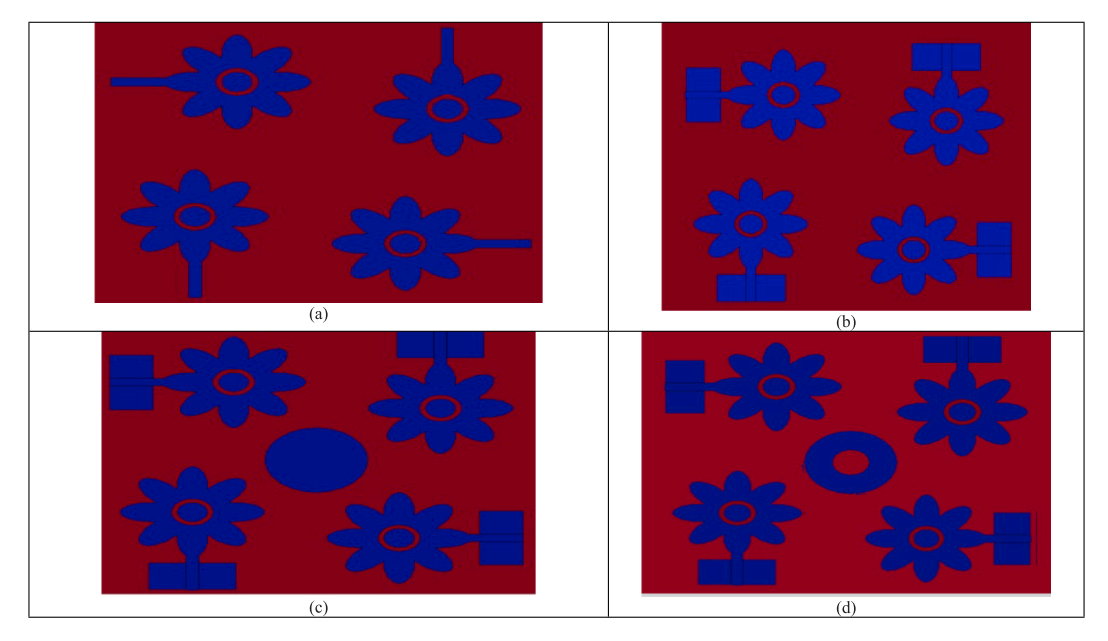


Fig. 2. Design evolution process of 4 \times 4 flower shaped UWB MIMO antenna.

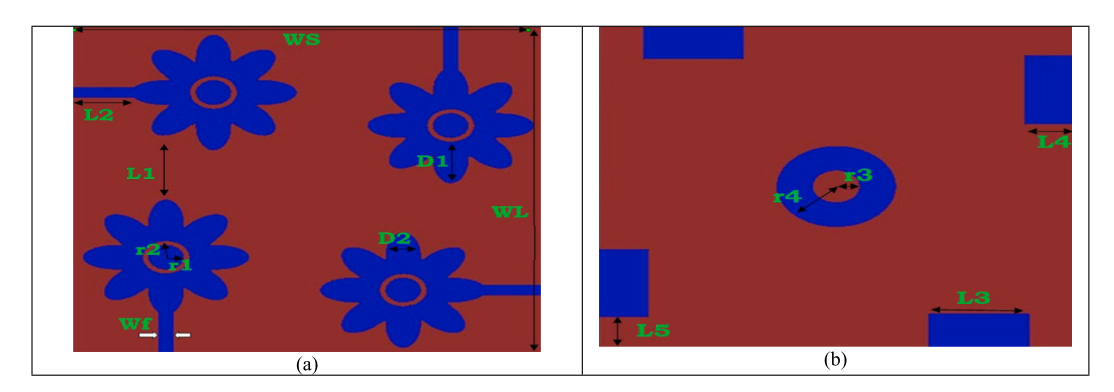


Fig. 3. Designed antenna (a) Top view (b) Bottom view.

ground of radiator A#0. The dimensions of ground brick length is 8.3 mm and width is 4.2 mm. The resultant antenna is called A#1. Now analyze characteristic modes of A#1.Ten modes are produced in all. While CM2, CM4, CM5, and CM6 are found in mid-band frequencies (4) GHz-8 GHz), the characteristic mode CM7 is resonated at 3.1 GHz [28]. Only mid-band frequencies are suitable for the Antenna A#1. High and low band frequencies are not appropriate for this antenna (A#1). Fig. 4 (b) represents the modal significances of A#1. Analyze the S-Parameters of antenna A#1 after applying an excitation pulse. Fig. 5 (b) shows the respective S-parameters of antenna A#1. A circular conduction patch with a 5 mm radius (r4) is positioned in the ground plane's center. The produced antenna that is known as A#2. Examine the A#2 CMS. For A#2, a total of 10 CMs are produced. The CM6 and CM7 are resonated at 3.1 GHz and 2.5 GHz low frequencies (1 GHz-4 GHz). The CM1, CM2 and CM4 are located at bid band frequencies (4 GHz-8 GHz). The CM5 and CM8 are resonated at 8.8 GHz and 9.2 GHz (Mid band frequencies). The remaining CMs CM3,CM9 and CM10 are not useful. These modes did not contribute any band width. This antenna A#2 is good at mid band and high band frequencies. The modal significances of A#2 are illustrated in Fig. 4.(c). Apply excitation signal to antenna A#2 and analyze its S-Parameters. The respective S-Parameters of antenna A#2 are depicted in Fig. 5 (c). Remove a circular conducting patch with a radius of (r3) 2 mm from antenna A#2 at the midpoint of the ground plane resulting antenna is called A#3. Anayze CMs of antenna A#3 using multi layer solver. Out of ten CMs CM1,CM2,CM4,CM6 are resonated at 5.2 GHz,6.5 GHz,5.1

GHz and 4.1 GHz (mid band frequencies) respectively [29]. The CM7 is resonated at 2.5 GHz (low frequencies). The CMs CM5, CM8 are resonated at 8.8 GHz and 9 GHz (High frequencies) respectively. The remaining CMs CM3, CM9 and CM10 did not contribute any bandwidth.

The modal significance of antenna A#3 are depicted in Fig. 4.(d). Apply excitation signal to antenna A#3 and analyze its S-Parameters. The S-Parameters of antenna A#3 are visualized in Fig. 5(d).All Characteristic modes in A#3 are scattered among low, Mid and high frequencies in the UWB spectrum. The Characteristic current distribution of CM4 in antennas A#1, A#2 and A#3 are analyzed at 5.1 GHz,6.5 GHz,7.5 GHz and 8.8 GHz and corresponding Current distribution are visualized in Fig. 6,Fig. 7 and Fig. 8..[30,31].

4. Result analysis OF 4 \times 4 flower-shaped MIMO-antenna

The radiator at port 1 is positioned perpendicularly to the radiators at ports 2, port 3, and 4.By creating polarization diversity with this configuration; the elements' isolation is improved. The constructed prototype, which was shown in Fig. 9. Measurements were obtained from port 1 using a four-port Vector Network Analyzer, with the remaining three ports yielding identical results because of the symmetry of the design.

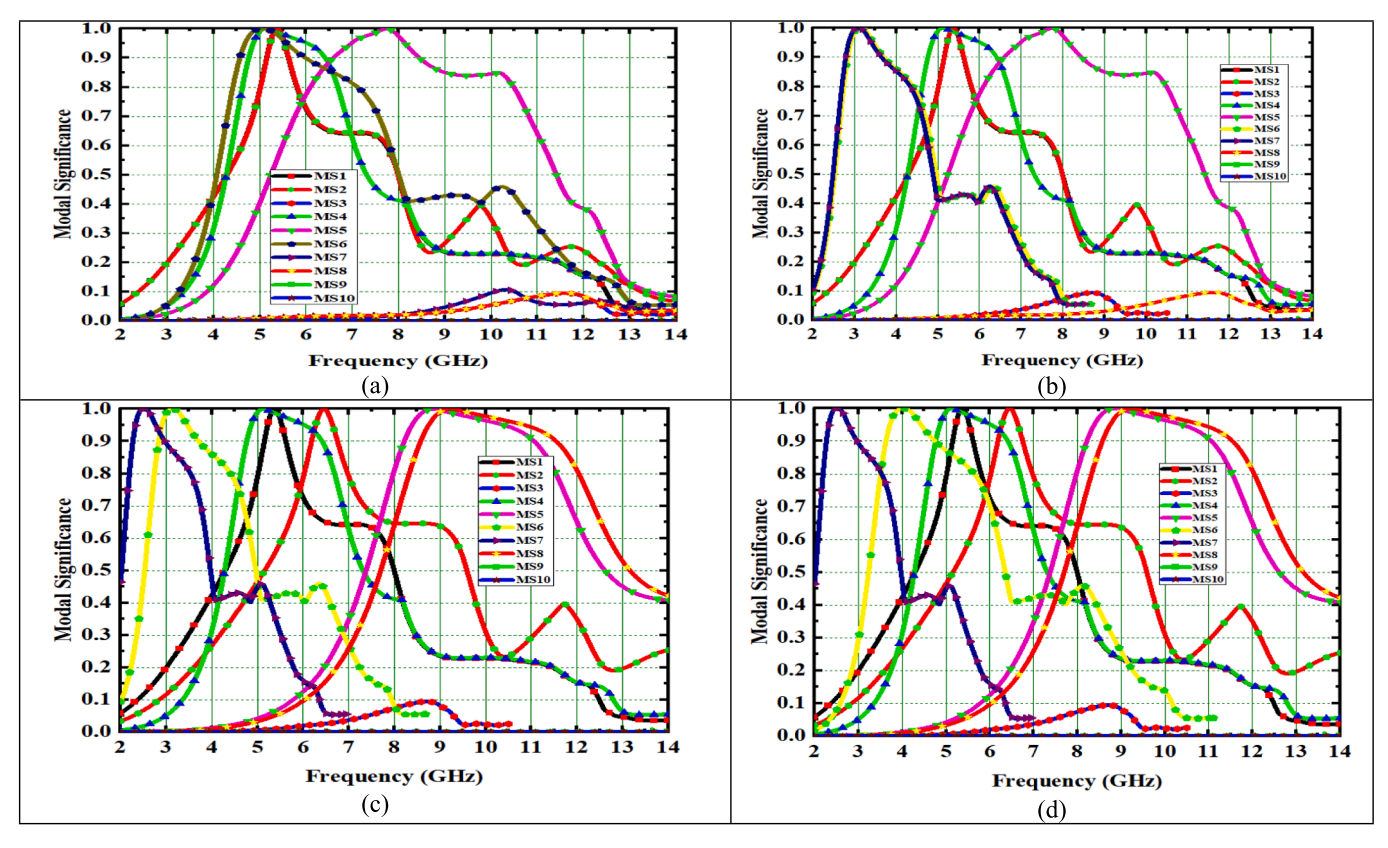


Fig. 4. Modal significances of (a) A#0 (b) A#1 (c)A#2 (d) A#3.

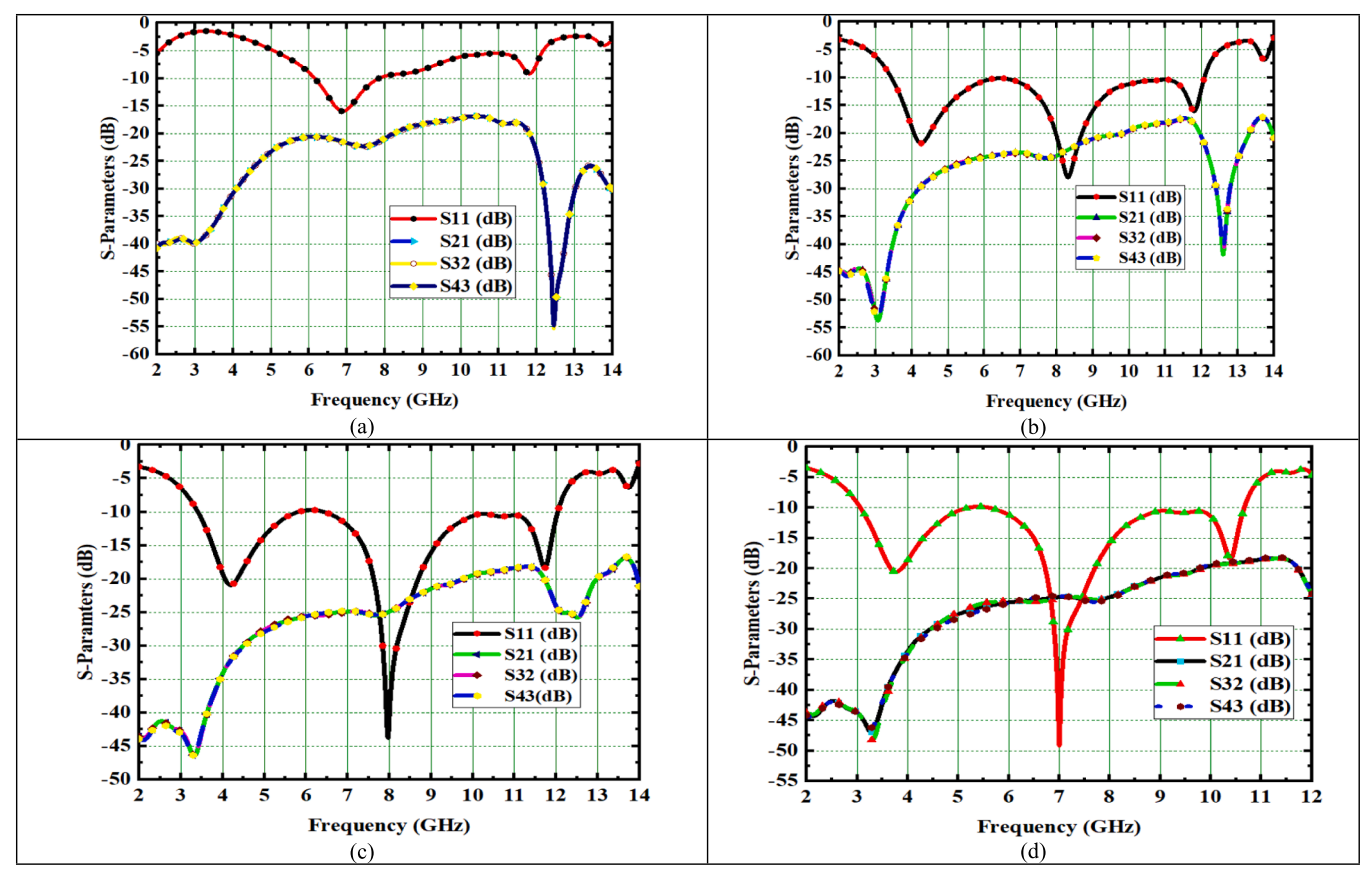


Fig. 5. S-paramters of 4 \times 4 Flower shaped antennas (a) A#0(b) A#1 (c) A#2 (d) A#3.

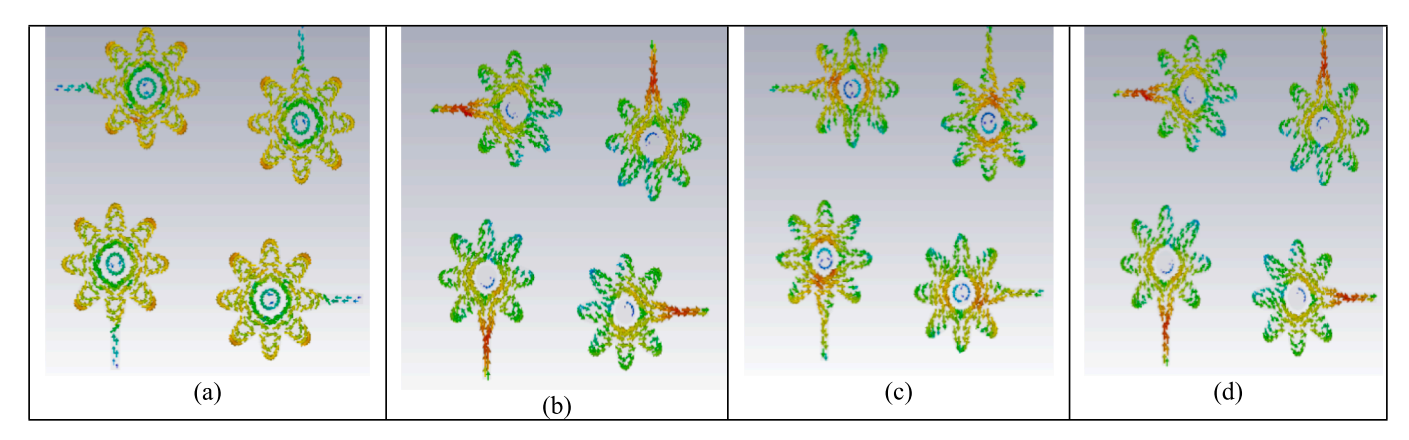


Fig.6. The Characteristic current distribution in A#1 of CM4 at (a) 5.1 GHz (b)6.5 GHz (c) 7.5 GHz (d) 8.8 GHz.

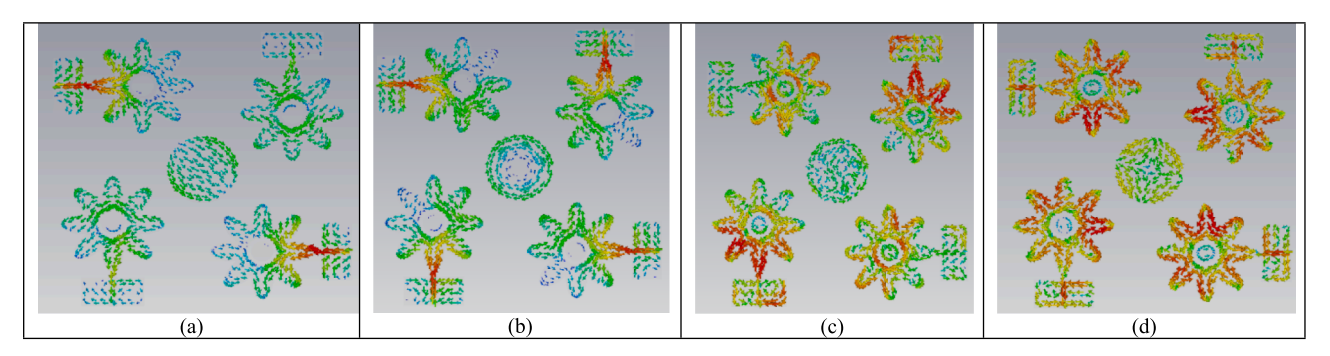


Fig. 7. The Characteristic current distribution in A#2 of CM4 at (a) 5.1 GHz (b)6.5 GHz (c) 7.5 GHz (d) 8.8 GHz.

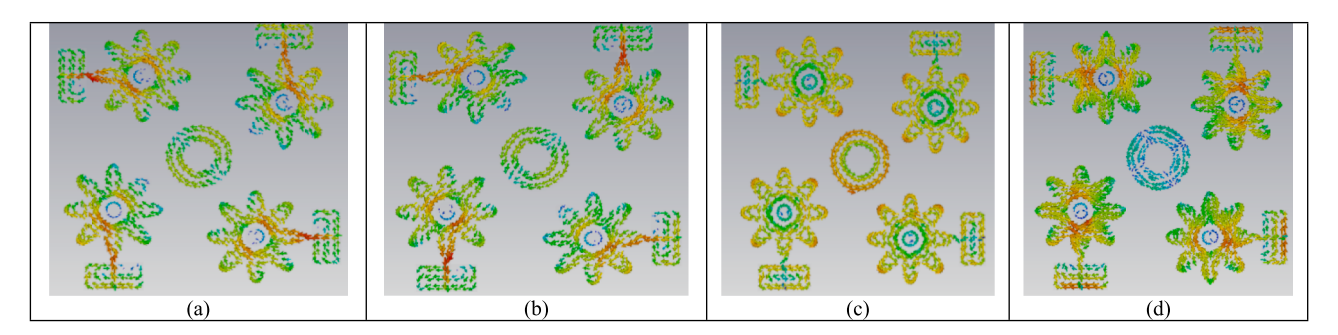


Fig. 8. The Characteristic current distribution in A#3 of CM4 at (I) 5.1 GHz (II) 6.5 GHz (III) 7.5 GHz (IV) 8.8 GHz.

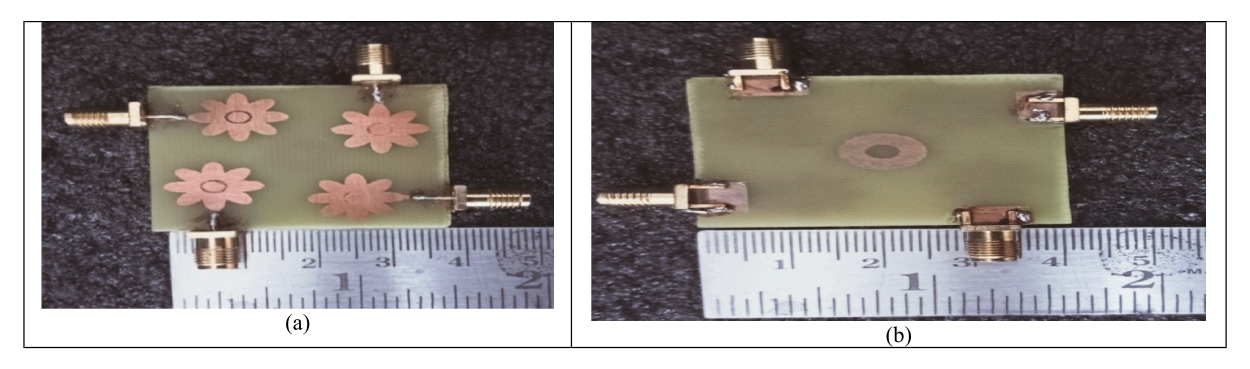


Fig. 9. Fabricated 4×4 flower shaped UWB MIMO antenna (a) Front View (b) Back View.

4.1. S-paramters

Fig. 10 shows the outputs of the desired MIMO antenna at port-1. The

simulated performance demonstrates a bandwidth of 7.9 GHz covering 3.1 to 11 GHz with $S_{11} \leq -10$ dB, while the tested results are nearly identical, offering an IBW of 112.8 %.The proposed antenna well

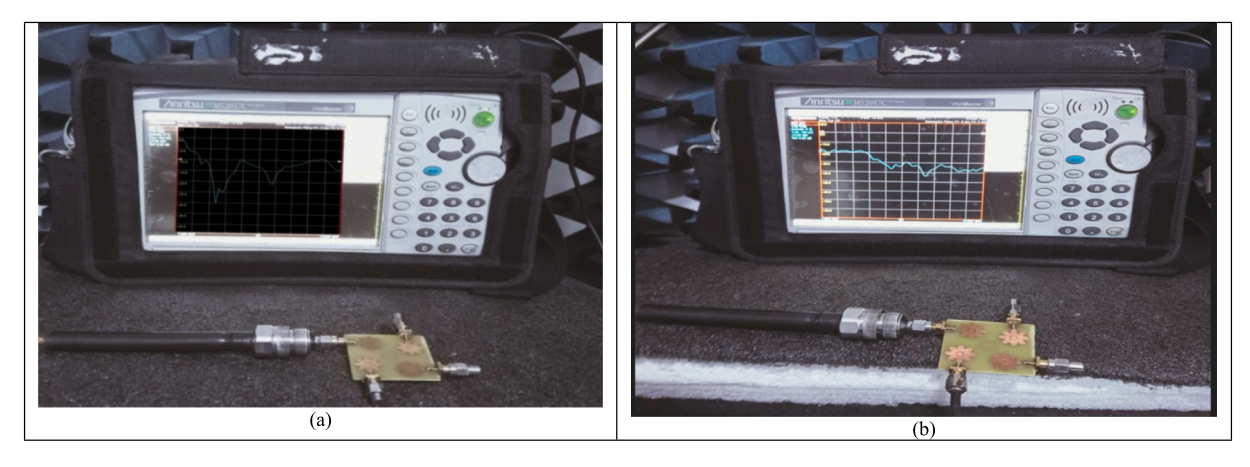


Fig. 10. Measurment of (a) return losses and (b)Isolation.

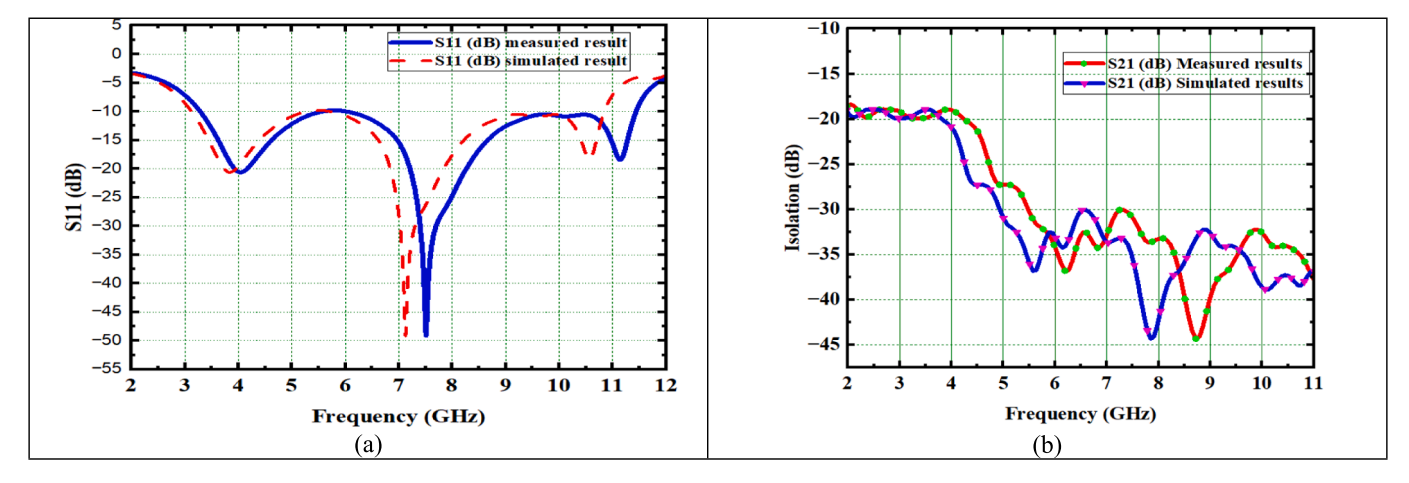


Fig. 11. Comparision of Simulated and tested (a) reflection coefficient (b) mutual coupling.

resonated at 4.1 GHz.

The proposed antenna achieved isolation $S_{21} < -26$ dB in entire UWB spectrum. The measured results of S_{11} and S_{21} are represented in Fig. 10 (a) and Fig. 10(b) respectively. Since the four radiating elements are identical, the S_{11} at all ports are same. Additionally, Fig. 10 demonstrates that the lasting three ports are linked to a 50 Ω load when the selected port is active. In addition, the achievement of a 90° phase difference among the ports confirms polarization diversity and strengthens the MIMO scheme.

The outcomes of simulation & experimental results for the S_{11} and S_{21} were displayed in Fig. 11(a) & Fig. 11(b), align well. Nevertheless, a small divergence amongst the simulated and measured outcomes is seen due to soldering. The antenna design with separate ground plane having some limitations. The impedance matching and fabrication process in antennas designed with separate ground planes are difficult. Due to ground plane interference, the Proposed MIMO antenna has less isolation

4.2. Radiation patterns

Measurements of co & cross-polarization at 4.1 GHz and 7.5 GHz were conducted in an anechoic chamber, as illustrated in Fig. 12 and show the 2-D radiation patterns of the proposed MIMO antenna shown in XZ & YZ planes at 4.1 GHz and 7.5 GHz. The measured and simulated results are visualized in Fig. 12. The practical and simulated radiation patterns exhibited omnidirectional &quasi-bidirectional actions in the H & E plane.

The radiation efficiency and gain, shown in Fig. 13, were 90 % and

5.5 dB, respectively. Fig. 13 presents the antenna's simulated and measured gain across varying frequencies, with the high gain of 5.5dBi. Fig. 14(a) and Fig. 14 (b) are displayed the 3D radiation outline results at 4.2 GHz and 7.5 GHz to validate the pattern diversity.

4.3. Diversity characteristics

The suggested MIMO antenna diversity properties are examined. In MIMO setups, the ECC measure the extent of interference linking between the MIMO elements. The DG which is related to the ECC describes the signal-to-interference ratio. The ECC threshold is under 0.5, while the DG threshold is approximately 10 dB. In MIMO antenna systems, ECC serves as a crucial parameter for assessing channel isolation, which is vital for maximizing channel capacity. While the ideal ECC value is zero, a practical target is to keep it below 0.5. ECC can be determined from the radiated fields between the ith and jth antennas, as outlined in equation (6) [32].

$$\rho_{e,ij} = \frac{\left| \iint_{4\pi} [E_i(\theta,\phi)]^* E_j(\theta,\phi) d\Omega \right|^2}{\iint_{4\pi} |E_i(\theta,\phi)|^2 d\Omega \iint_{4\pi} |E_j(\theta,\phi)|^2 d\Omega}$$
(6)

Here, $E_i(\theta, \varphi)$ represents the radiation of the i^{th} antenna. The computed ECC for antenna elements 1 and 2, calculated using the equations in (6), is shown in Fig. 15. As the design is symmetrical, ECC results for all other elements will be similar. If a lossless isotropic environment is assumed, ECC computation from S-parameters can be performed using equation (7) [33]. S-parameters and far-field measurements are used to assess the desired antenna's ECC. With the use of the CMA approach, the suggested

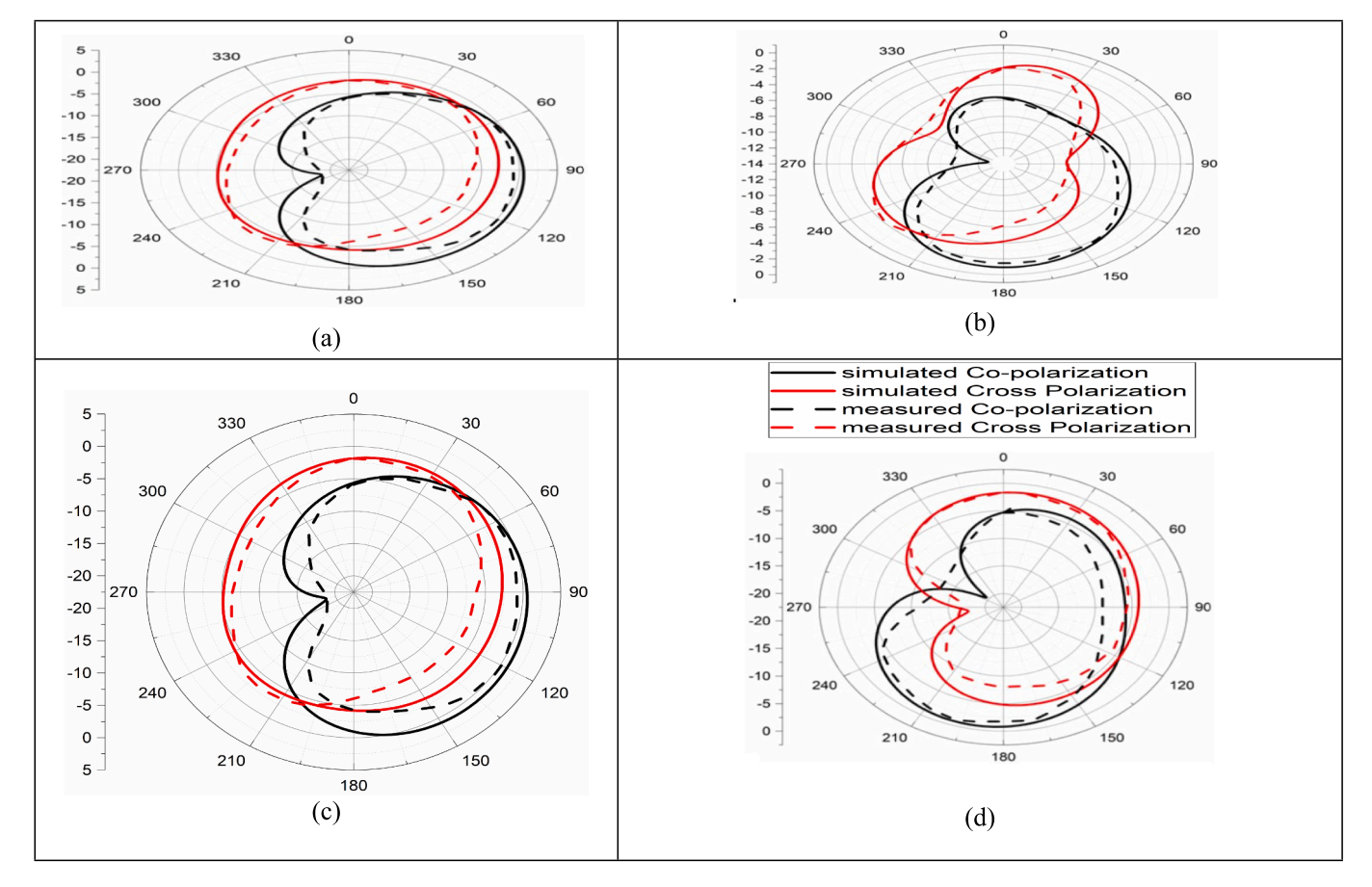


Fig. 12. The flower-shaped 4 × 4 MIMO Antenna Co and Cross polarization of E-Plane at(a)4.1 GHz,(c) 8.7 GHz and H-plane at(b) 4.1 GHz (d)8.7 GHz.

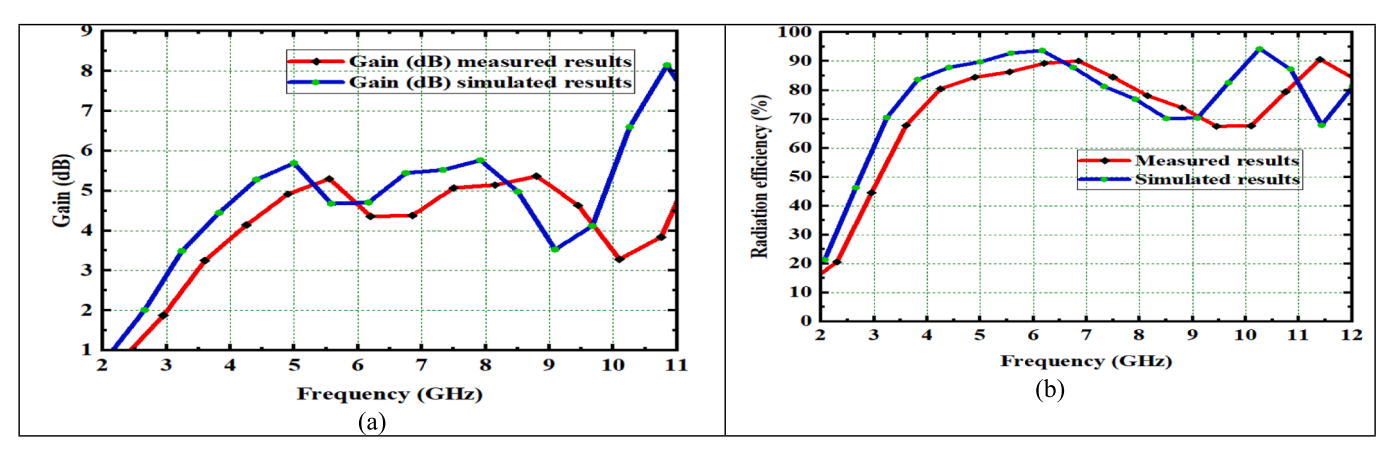


Fig. 13. (a) Gain (b) Radiation efficiency.

antenna achieved an ECC of 0.0016, as shown in Fig. 15(b).

$$\rho_e(i,j,4) = \frac{\left|\sum_{n=1}^4 S_{i,n}^* S_{n,j}\right|^2}{\prod_{k=i,j} \left[1 - \sum_{n=1}^4 S_{i,n}^* S_{n,k}\right]}$$
(7)

By incorporating antenna elements that are fading at different rates, diversity techniques are used to lessen the impacts of fading. Equations (8) and (9) used to determine the DG of the antenna, which comes out to be about 10 dB [32]. The designed antenna achieved the Diversity gain nearly equals to 10 dB and depicted in Fig. 15. (a)

$$DG = 10\sqrt{1 - \rho_e^2} \tag{8}$$

$$DG = \left[\left(\frac{\gamma_c}{SNR_c} - \frac{\gamma_1}{SNR_1} \right)_{P(\gamma_c < \frac{\gamma_s}{SNR})} \right]$$
 (9)

4.3.1. MEG

MEG is an essential system of measurement for estimating MIMO diversity. When there is fading, it shows power difference as compared to an isotropic antenna. As illustrated in Fig. 16(a), the proposed MIMO achieved a MEG of -3.3 dB. The MEG calculation follows equation (10) and equation (11) [34]

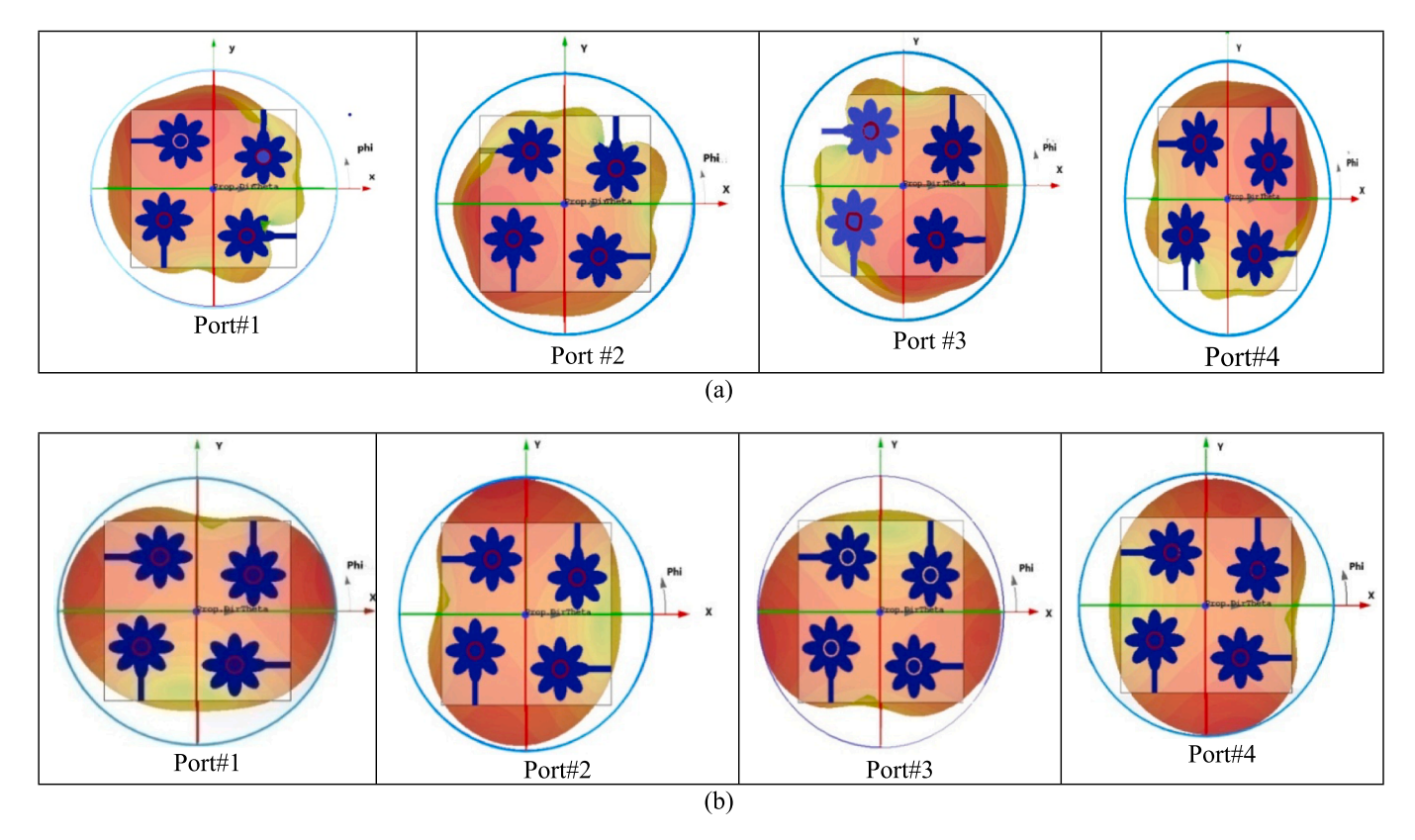


Fig. 14. 3D radiation pattern of flower shaped MIMO antenna at (a) 4.2 GHz and (b) 7.5 GHz.

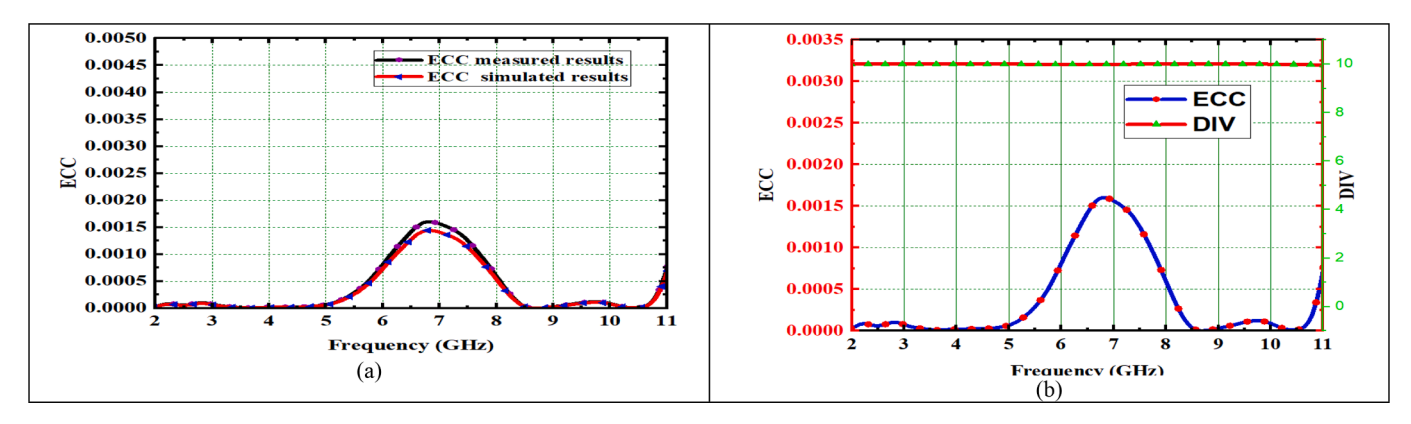


Fig. 15. Simulated and measured (a) ECC (b) diversity gain.

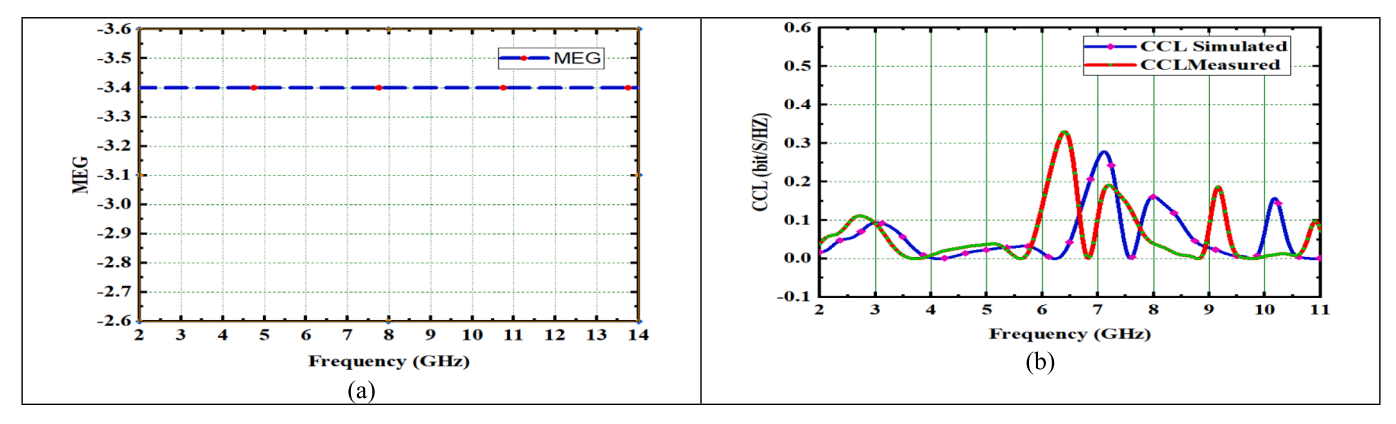


Fig. 16. (a) MEG (b) CCL.

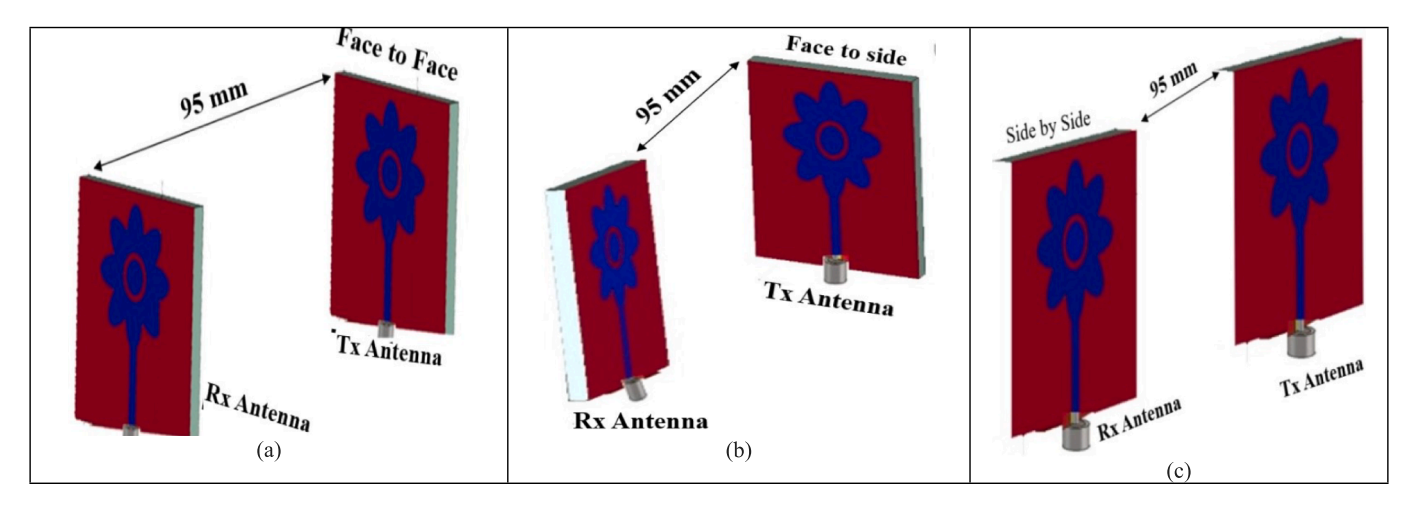


Fig. 17. Time-domain analysis setup for (a) Face to face (b) face to side (c)side by side.

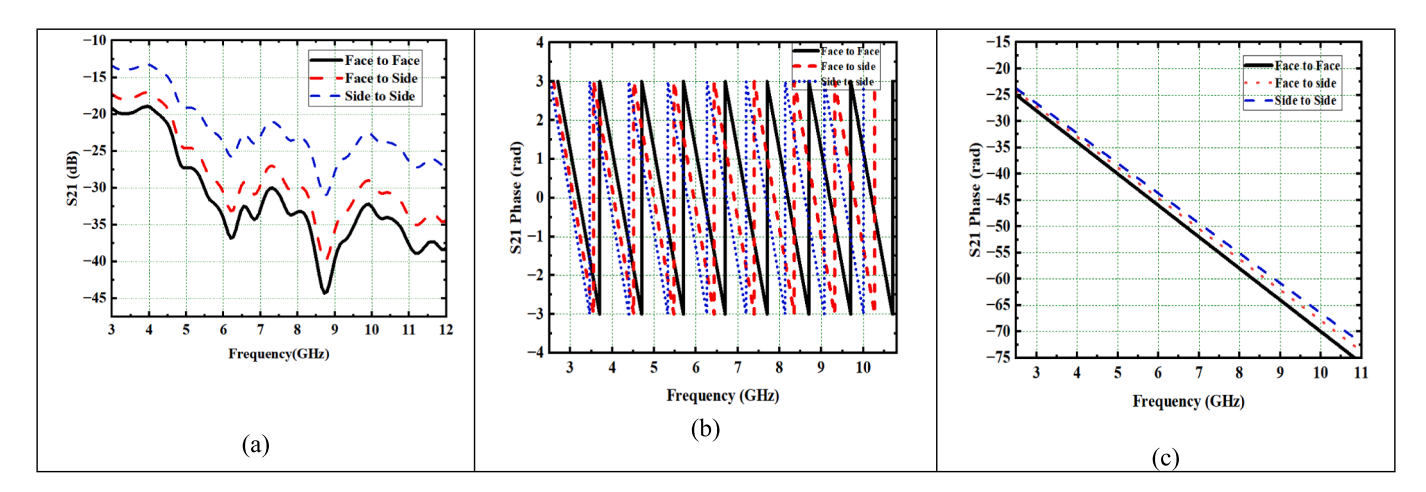


Fig. 18. Simulated outcomes for various layouts showing (a) S₂₁, (b) S₂₁ phase, and (c) unwrapped S₂₁ phase.

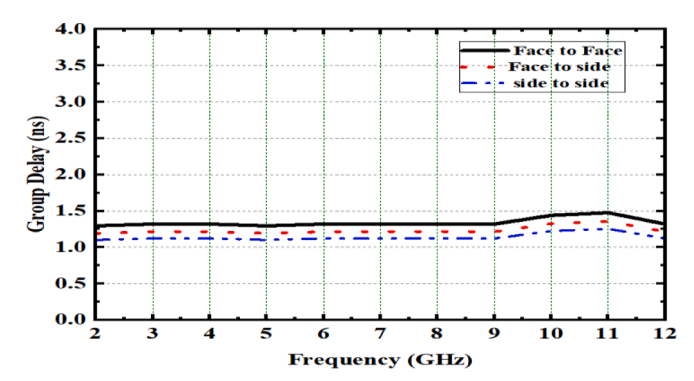


Fig. 19. Group delay.

$$MEG_i = 0.5(1 - \sum_{j=1}^{k} |S_{ij}|^2$$
 (10)

The MEG is expressed

$$\begin{split} \textit{MEG} &= \int_{0}^{2\pi} \int_{0}^{\pi} \left[\frac{\textit{XPR}}{1 + \textit{XPR}} F_{\alpha}(\alpha, \beta) P_{\alpha}(\alpha, \beta) \right. \\ &+ \frac{1}{1 + \textit{XPR}} F_{\beta}(\alpha, \beta) P_{\beta\Phi}(\alpha, \beta) \left[\sin \alpha d\alpha d\beta \right] \end{split} \tag{11}$$

In the MIMO antenna system, F_{α} and F_{β} denote the power patterns. The

MEG in these types of systems is typically less than -3 dB between two ports. The MEG relating port 1 and port 3 for the proposed 4×4 antenna is -3.3 dB, represented in the Fig. 16(a).

4.3.2. CCL

In MIMO antenna systems, the CCL is a central factor for assessing radiation performance. In MIMO schemes, 0.4 bits/s/Hz is the accepted lower bound for CCL. The equations (12)–(14) [34] contain its mathematical definition.

$$C_{loss} = -log_2 det(\rho^R)$$
 (12)

$$B = \begin{bmatrix} \rho_{11} & \rho_{12} & \rho_{13} & \rho_{14} \\ \rho_{21} & \rho_{22} & \rho_{23} & \rho_{24} \\ \rho_{31} & \rho_{32} & \rho_{33} & \rho_{34} \\ \rho_{41} & \rho_{42} & \rho_{42} & \rho_{44} \end{bmatrix}$$
(13)

And also expressed asB_{nm} =
$$-(S_{nn}^*S_{nm} + S_{mn}^*S_{nm})$$
 (14)

In this case, n and m range from 1 to 4. Fig. 16(b) presents the simulated and observed CCL values. Across the full UWB frequency range, the antenna design attained a CCL of $0.32\ bits/s/Hz$.

5. Time-domain study of flower shaped antenna

The proposed design working is assessed using time-domain analysis. In UWB technology, it transmits narrow pulses, leading to a wide-band

Table 3Comparison among proposed work and other selected designs.

| Ref | Dimensions (mm ³) | Gain (dBi) | Efficiency (%) | Isolation (dB) | ECC | DG |
|--------|-------------------------------|------------|----------------|----------------|----------|------|
| [29] | $40 \times 40 \times 1.6$ | 5.5 | >89 | <-18 | < 0.012 | 9.89 |
| [30] | $40 \times 40 \times 1.6$ | 5.6 | >90 | <-25 | < 0.0045 | 9.92 |
| [31] | $40 \times 40 \text{x} 1.6$ | 4.9 | >89 | <-26 | < 0.0016 | 9.92 |
| [36] | $93x93 \times 1.6$ | 5.4 | 82 | <-20 | < 0.003 | >9.8 |
| [37] | 30 	imes 30 	imes 1.6 | 6.2 | 87 | <-17 | < 0.001 | >9.9 |
| [38] | 40 × 40 | 8.5 | 76 | <-27 | _ | _ |
| [39] | $56 \times 68 \times 0.2$ | 5.87 | _ | <-15 | < 0.02 | >9.9 |
| [40] | $80 \times 80 \times 1.6$ | 5.8 | 80 | <-25 | < 0.02 | >9.9 |
| [41] | $40 \times 40 \times 1.6$ | 3.5 | 77 | <-16 | < 0.1 | >9.9 |
| [Prop] | $40\times40\times1.6$ | 5.5 | 90 | <-26 | 0.0016 | 9.99 |

response in the frequency domain. Key parameters such as time-domain features, the transmission coefficient (S_{21}), the phase of S_{21} , and group delay are crucial for demonstrating the antenna's suitability for UWB applications. Fig. 17 depicts the single antenna configurations for three distinct arrangements: face-to-face(f-f), face-to-side(f-s), and side-by-side(s-s). A pair of identical antennas are arranged in three different ways, with a gap of 95 mm between them. The transmitter (Tx) and receiver (Rx) are represented by one and one antenna, respectively. Fig. 18 shows the magnitude, phase, and unwrapped phase of S_{21} .

 S_{21} values for all three antenna configurations exhibit consistent performance from 3.1 to 10.6 GHz, staying below -26 dB throughout the frequency range, as shown in Fig. 18(a). Particularly in the f-f and f-s configurations, the values drop to below -35 dB at higher frequencies, between 11 and 12 GHz. Fig. 18(b) displays the S_{21} phase, while Fig. 18 (c) shows the unwrapped phase to provide a clearer view of the linear characteristics throughout wide band operation. Group delay results are presented in Fig. 19. With a small variation of about 0.1 ns near the end of the band, particularly in the f-f and f-s configurations, the group delay stays constant at roughly 1.1 ns across the operational range.

The suggested antenna's time-domain study showed linear transmission properties, including a constant group delay and low transmission coefficient throughout the working region. The following equation (15)[35] provides an explanation of the time domain analysis

$$x(t) = A\left(-\frac{15t}{\sqrt{2\pi\sigma^7}} + \frac{10t^3}{\sqrt{2\pi\sigma^9}} - \frac{t^5}{\sqrt{2\pi\sigma^{11}}}\right) x e^{\frac{-t^2}{2\sigma^2}}$$
 (15)

In Equation (15), 't' stands for time, 'A' indicates amplitude, and 's' refers to the spread of the Gaussian pulse.

6. Comparisions with existing models

The proposed working model is compared to existing models [29–3136–41] based on factors such as size, bandwidth, gain, and diversity parameters like ECC, MEG, CCL, and radiation characteristics. The comparative analysis demonstrates that the suggested antenna, with CMA and a systematic design, enhances diversity metrics like ECC, DG, and CCL across the entire UWB range. The flower-shaped 4×4 UWB-MIMO antenna was engineered to operating the UWB frequencies. It offers several improvements over previously reported designs in the literature [29–41], as shown in Table 3. Compared to standard models, the proposed antenna incorporates the advantage of the CMA method. Its ECC, IBW, and diversity performance have been observed to be excellent.

7. Conclusions

The frequency range that the flower-shaped UWB- MIMO antenna works in 3.1 GHz to 11 GHz. Significantly below 26 dB is the isolation between radiating parts, and return losses are less than 10 dB. The radiation parameters include a gain of 5.5 dB, an IBW of 117.15 %, and 90 % efficiency. ECC, DG, MEG, and CCL have diversity metrics of 0.0016, 9.982 dB, -3.3 dB, and 0.32 bits/s/Hz, accordingly. Through

sophisticated experimentation, these findings have been validated. The desired MIMO antenna is a suitable for wireless communication in UWB applications based on its operational characteristics.

CRediT authorship contribution statement

Ankireddy Chandra Suresh: Writing – original draft, Software, Methodology, Conceptualization. Chandraiah.G: Writing – original draft, Software, Methodology, Conceptualization. Chiranjeevi Althi: Writing – original draft, Software, Methodology, Conceptualization. Om Prakash Kumar: Writing – review & editing, Supervision, Conceptualization. Moath Alathbah: Writing – original draft, Software, Methodology, Conceptualization. BTP Madhav: Writing – review & editing, Supervision, Methodology, Conceptualization.

Declaration of competing interest

The authors declare that they have no known competing financial interests or personal relationships that could have appeared to influence the work reported in this paper.

Acknowledgements

The authors would like to acknowledge the support provided by researchers supporting project number (RSPD2024R868), King Saud University, Riyadh, Saudi Arabia, and DST through SR/FST/ET-II/2019/450 & SR/PURSE/2023/196.

Data availability

The data used to support the findings of this study are included in the article.

References

- [1] Federal Communications Commission (FCC)., Revision of Part 15 of the Commission's Rules Regarding Ultra-Wideband Transmission Systems First Rep. and Order, ET Docket 98-153, FCC 02-48, Adopted: Feb 2002; Released; 2002.
- [2] Hasan MM, Faruque MRI, Islam MT. Dual band metamaterial antenna for LTE/bluetooth/WiMAX system. Sci Rep 2018;8:1240.
- [3] Amin F, Saleem R, Shabbir T, Rehman SU, Bilal M, Shafique MF. A compact quadelement UWB-MIMO antenna system with parasitic decoupling mechanism. Appl Sci 2019:9:2371.
- [4] Nadeem I, Choi D-Y. Study on mutual coupling reduction technique for MIMO antennas. IEEE Access 2018;7:563–86.
- [5] Haq MAU, Koziel SJ. Ground plane alterations for design of high-isolation compact wideband MIMO antenna. IEEE Access 2018;6:48978–83.
- [6] Tang Z, Wu X, Zhan J, Hu S, Xi Z, Liu Y. Compact UWB-MIMO antenna with high isolation and triple band-notched characteristics. IEEE Access 2019;7:19856–65.
- [7] Wu A, Zhao M, Zhang P, Zhang Z. A compact four-port MIMO antenna for UWB applications. Sensors 2022;22(15):5788.
- [8] Babu KV, Anuradha B. Design of MIMO antenna to interference inherent for ultra wide band systems using defected ground structure. Microw Opt Technol Lett 2019;61(12):2698–708.
- [9] Sree GNJ, Nelaturi S. Opportunistic control of fractal-based MIMO antenna for sub-6-GHz 5G applications. Int J Commun Syst 2021;34(17):e4991.

- [10] Ibrahim AA, Ahmed MI, Ahmed MF. A systematic investigation of four ports MIMO antenna depending on flexible material for UWB networks. Sci Rep 2022;12(1): 14351
- [11] Saadh AM, Ramaswamy P, Ali T. A CPW fed two and four element antenna with reduced mutual coupling between the antenna elements for wireless applications. Appl Phys A 2021;127(2):88.
- [12] Khan MA, Al Harbi AG, Kiani SH, Nordin AN, Munir ME, Saeed SI, et al. mmWave four-element MIMO antenna for future 5G systems. Appl Sci 2022;12(9):4280.
- [13] Kiani SH, Alharbi AG, Khan S, Marey M, Mostafa H, Khan MA. Wideband three loop element antenna array for future 5G mmWave devices. IEEE Access 2022;10: 22472-9.
- [14] Kiani SH, Savci HS, Munir ME, Sedik A, Mostafa H. An ultra-wide band MIMO antenna system with enhanced isolation for microwave imaging applications. Micromachines 2023;14(9):1732.
- [15] Alharbi AG, Rafique U, Ullah S, Khan S, Abbas SM, Ali EM, et al. Novel MIMO antenna system for ultra wideband applications. Appl Sci 2022;12(7):3684.
- [16] Saad AAR, Mohamed HA. Conceptual design of a compact four-element UWB MIMO slot antenna array. IET Microwaves Antennas Propag 2019;13(2):208–15.
- [17] Yang L, Xu M, Li C. Four-element MIMO antenna system for UWB applications. Radioengineering 2019;28(1):60–7.
- [18] Kayabasi A, Toktas A, Yigit E, Sabanci K. Triangular quad-port multi-polarized UWB MIMO antenna with enhanced isolation using neutralization ring. AEU-Int J Elect Commun 2018;85:47–53.
- [19] A. Desai, J. Kulkarni, M.M. Kamruzzaman, S. Hubálovský, H.-T. Hsu, A.A. Ibrahim, Interconnected CPW Fed Flexible 4-Port MIMO Antenna for UWB, X, and Ku Band Applications. IEEE Access 2022, 10, 57641–57654.ACCESS.2022.3179005.
- [20] Shi C, Zhao Z, Du C. A design of quad-element dual-Band MIMO antenna for 5G application. Micromachines 2023;14(7):1316.
- [21] Baz A, Jansari D, Lavadiya SP, Patel SK. Miniaturized and high gain circularly slotted 4× 4 MIMO antenna with diversity performance analysis for 5G/Wi-Fi/ WLAN wireless communication applications. Results Eng 2023;20:101505.
- [22] Pandya K, Upadhyaya T, Patel U, Sorathiya V, Pandya A, Al-Gburi AJA, et al. Performance analysis of quad-port UWB MIMO antenna system for Sub-6 GHz 5G, WLAN and X band communications. Results Eng 2024:102318.
- [23] Kumar P, Pathan S, Vincent S, Kumar OP, Yashwanth N, Kumar P, et al. A compact quad-port UWB MIMO antenna with improved isolation using a novel mesh-like decoupling structure and unique DGS. IEEE Trans Circuits Syst Express Briefs 2022; 70(3):949–53.
- [24] Rekha VSD, Pardhasaradhi P, Madhav BTP, Devi YU. Dual band notched orthogonal 4-element MIMO antenna with isolation for UWB applications. IEEE Access 2020;8:145871–80.
- [25] Khan AA, Naqvi SA, Khan MS, Ijaz B. Quad port miniaturized MIMO antenna for UWB 11 GHz and 13 GHz frequency bands. AEU-Int J Elect Commun 2021;131: 153618.
- [26] Kumar P, Pathan S, Kumar OP, Vincent S, Nanjappa Y, Kumar P, et al. Design of a six-port compact UWB MIMO antenna with a distinctive DGS for improved isolation. IEEE Access 2022;10:112964–74.

- [27] Kempanna SB, Biradar RC, Kumar P, Kumar P, Pathan S, Ali T. Characteristic-mode-analysis-based compact vase-shaped two-element uwb mimo antenna using a unique dgs for wireless communication. J Sensor Actuator Networks 2023;12(3). 47 Equation [1-5].
- [28] Singh HV, Tripathi S. Compact UWB MIMO antenna with Fork-shaped stub with vias based coupling current steering (VBCCS) to enhance isolation using CMA. AEU-Int J Elect Commun 2021;129:153550.
- [29] Suresh AC, Reddy T. S,"A flower shaped miniaturized 4x 4 MIMO antenna for UWB applications using characteristic mode analysis. Progress Elect Research C 2022:119.
- [30] Suresh AC, Reddy TS, Madhav BTP, Das S, Lavadiya S, Algarni AD, et al. Investigations on stub-based UWB-MIMO antennas to enhance isolation using characteristic mode analysis. Micromachines 2022;13(12):2088.
- [31] A.C. Suresh, T.S. Reddy, B.T.P. Madhav, S. Alshathri, W. El-Shafai, S. Das, V. Sorathiya, "A Novel Design of Spike-Shaped Miniaturized 4× 4 MIMO Antenna for Wireless UWB Network Applications Using Characteristic Mode Analysis," Micromachines, 14(3), 612, 2023.
- [32] Y.A.S. Dama, R.A. Abd-Alhameed, S.M.R. Jones, D. Zhou, N.J. McEwan, M.B. Child, P.S. Excell, (2011). An envelope correlation formula for (N, N) MIMO antenna arrays using input scattering parameters, and including power losses. international journal of antennas and propagation, 2011(1), 421691.(equation ECC)
- [33] Thaysen J, Jakobsen KB. Envelope correlation in (N, N) MIMO antenna array from scattering parameters. Microw Opt Technol Lett 2006;48(5):832–4 (ECC).
- [34] Suresh AC, Reddy TS. Experimental investigation of novel frock-shaped miniaturized 4× 4 UWB MIMO antenna using characteristic mode analysis. Progress in Elect Research B 2023;101:(MEG).
- [35] Addepalli T, Desai A, Elfergani I, Anveshkumar N, Kulkarni J, Zebiri C, et al. 8-Port semi-circular arc MIMO antenna with an inverted L-strip loaded connected ground for UWB applications. Electronics 2021;10(12):1476. Equation 15.
- [36] Gupta SK, Mark R, Mandal K, Das S. Four element UWB MIMO antenna with improved isolation using resistance loaded stub for S, C, and X band applications, Progress in Elect Research C 2023;131:73–87.
- [37] A.H. Jabire, S. Sani, S. Saminu, M.J. Adamu, M.I. Hussein," A crossed-polarized four port MIMO antenna for UWB communication," Heliyon, 9(1), 2023.
- [38] Althuwayb A. A "Low-interacted multiple antenna systems based on metasurfaceinspired isolation approach for MIMO applications,. Arab J Sci Eng 2022;47(3): 2629–38.
- [39] Desai A, Kulkarni J, Kamruzzaman MM, Hubálovský Š, Hsu HT, Ibrahim A. A, "Interconnected CPW fed flexible 4-port MIMO antenna for UWB, X, and Ku band applications., IEEE Access 2022;10:57641–54.
- [40] Rekha VSD, Pardhasaradhi P, Madhav BTP, Devi Y. U,"Dual band notched orthogonal 4-element MIMO antenna with isolation for UWB applications,. IEEE Access 2020;8:145871–80.
- [41] Abdelghany MA, Sree MFA, Desai A, Ibrahim AA. 4-Port octagonal shaped MIMO antenna with low mutual coupling for UWB applications. CMES-Comput Model Eng Sci 2023;136(2):1999–2015.